Quasi-static PZT actuated MEMS mirror with 4x3mm^2 reflective area and high robustness

N. Boni[a*], R. Carminati[a], G. Mendicino[a], M. Merli[a]
[a]STMicroelectronics, AMS Group, Via Tolomeo 1, Cornaredo, Milan, Italy 20010

ABSTRACT

Piezoelectric thin films have gained attention as key materials for the actuation of micro devices since they provide high drive forces compared to others actuation mechanisms. One of the most challenging application field is the design of quasi-static MEMS scanners, in which is difficult to have a high torsional angle and large reflective area while maintaining a good device robustness. In this work a monoaxial, quasi-static MEMS mirror with PZT actuation will be presented, surpassing the limitations found in the state-of-the-art solutions. The mirror has a large reflective area in the visible spectrum (4x3mm with aluminum coating) and the half mechanical opening angle is of 9deg (corresponding to a field of view of 36deg) with a relatively low actuation voltage (40V). To enable the mirror control, a diffused piezoresistive sensor in a Wheatstone bridge configuration is integrated in the technology platform. The innovative mirror design guarantees high resonant frequencies of the torsional mode (>500Hz) and higher spurious modes (>2.5kHz), which allow a quasi-static actuation for the typical display refresh rates (up to 120Hz). The high frequencies of the translational spurious modes guarantee a high robustness against shocks and vibrations, which makes this mirror suitable for consumer or automotive products. In this paper it will be described the working principle of the patented MEMS design, the manufacturing process, the FEM simulations and the experimental findings obtained on fabricated samples.

Keywords: MEMS scanner, MEMS mirror, quasi-static actuation, PZT, piezoelectric, AR/MR, LiDAR

1. INTRODUCTION

The adoption of MEMS mirrors has been rapidly growing in recent years, involving different types of applications: in the early 00s the main goal was to develop consumer pico-projectors, while more recently the main focus was related to AR/MR and LiDAR applications. MEMS laser projectors can be found, among others, in: North (now Google) Focals [1], Microsoft Hololens 2 [2], Bosch Smartglasses Light Drive module [3] for AR/MR applications and Intel RealSense L515 [4] and Innoviz One [5] for short and long range LiDAR. Additional examples of products including MEMS laser projectors, with an extensive description of the optical engines used can be found in [6].

All these use cases have in common the request of increasing the projection performances in terms of resolution, field of view (FOV) and refresh rate, which translates into the requirements of bigger reflective area of the mirrors, higher mechanical opening angles and higher working frequencies. For these reasons industry and researchers are developing new MEMS technologies that can provide such improvements.

The first MEMS mirrors developed in the past years used electrostatic actuation [7][8], a well-known actuation technique adopted in all kind of MEMS sensors and actuators, which can provide torque by means of comb fingers. The main disadvantages of electrostatic actuation are related to the high actuation voltage needed (up to 200V), which affect the power consumption of the system, and the limited projection performance that can be reached (usually up to 600p, 60Hz), due to the limited opening angle and device robustness achievable with this kind of technology.

Another actuation technology adopted in the past few years is based on Lorentz force (i.e. electromagnetic actuation), generated by an electrical current flowing in a movable coil placed in a static magnetic field [9][10]. The advantage of this actuation technology relies in the increased torque compared with electrostatic actuation, which can be used to increase the opening angle, mirror reflective area and robustness of the device. The drawbacks are related to the increased power consumption (high current flowing in the coil, usually hundreds of mA), the generation of the magnetic field which require bulky magnets and the possible reliability problems arising from exposed metal coils, which can affect the lifetime of the device or may require a weather sealing that can further increase the volume occupation of this solution.

* nicolo.boni@st.com

To overcome these limitations, in the past few years a big effort was made to develop MEMS technologies incorporating piezoelectric materials, which can provide high force with low power consumption and not requiring additional bulky elements in the assembly.

STMicroelectronics developed PεTRA technology [12], based on PZT material, to support the request of better and more efficient actuation common to all kind of MEMS actuators, including μlenses (partnership with Polight [13]), μspeakers (partnership with uSound [14]) and μmirrors.

One of the main challenges in MEMS mirrors is related to the "slow axis" quasi-static design, whether it is a biaxial or double monoaxial mirror solution: quasi-static mirrors don't take advantage of the the Q-factor amplification as in resonant mirrors and this require a low torsional stiffness and big torque (i.e. big actuators). In addition, quasi-static axis usually requires a big movable mass (big reflective area required for monoaxial design, gimbal and fast axis actuators carried by quasi-static axis in the biaxial approach, as highlighted in Figure 1), which can strongly affect the device robustness. This challenge is even more felt for piezoelectrically actuated micromirrors where few solutions reaching good scanning performances have been proposed up to now [15][16], but where still it can be recognized a risk of limited mechanical robustness.

This work will focus on a novel design concept of quasi-static MEMS mirrors with a big reflective area of 4x3mm^2, addressing such challenges and guaranteeing remarkable results in terms of performance and robustness. In Section 2 the design and the manufacturing process are described, Section 3 will show simulation results together with characterization and reliability measurements and Section 4 will conclude highlighting the main results obtained and the future possibilities that can be achieved using this kind of technology and design concept.

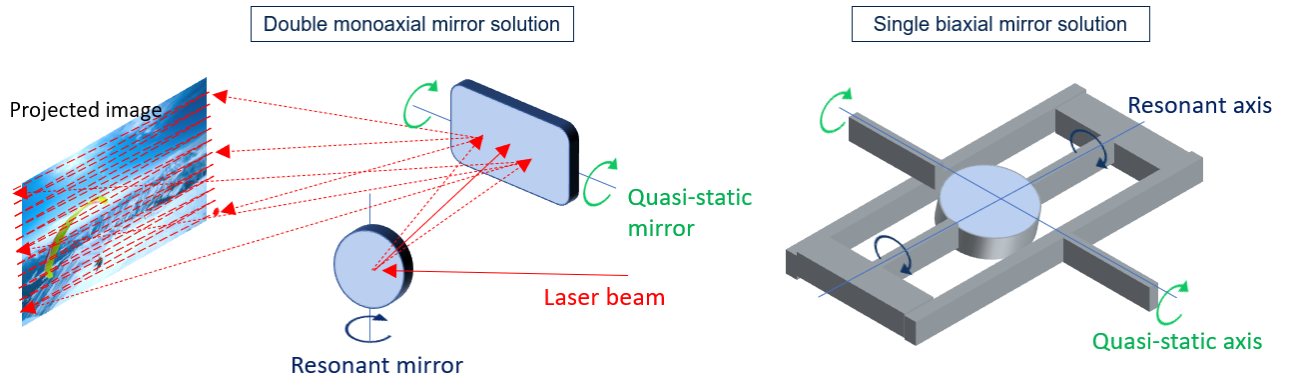

Figure 1 Double monoaxial (left) and single biaxial (right) projection solution. It can be noted that quasi-static axis, highlighted in green, requires bigger area and movable mass.

2. DESIGN AND PROCESS DESCRIPTION

In the world of piezoelectric thin films for MEMS there are several possible solution and the material selection has to be made depending on the MEMS requirements: as reference, one can compare 3 main materials used for actuation and sensing in MEMS: PZT, AlN and AlScN. Recalling what done in [15], in Table 1 are reported the main material properties that need to be considered during the design of a piezoelectric MEMS.

Table 1 Comparison between the main thin film materials used for MEMS actuation and sensing

Property	**PZT**	**AlN**	**AlScN**
$e_{31,f}$ [C/m^2] Piezoelectric coefficient	~15	~1	~2
Linearity	Nonlinear	Linear	Linear
ε_r [-] Relative permittivity	~1200	~10	~15
tanδ [%] Dielectric loss	~3	~0.03	~0.1

For MEMS mirrors (and more in general for all MEMS actuators) the most important parameter is the $e_{31,f}$, which is directly related to the force that the film is able to transfer to the silicon structure: as it can be noted, the PZT force is ~1 order of magnitude greater then AlN/AlScN and thus, to obtain the same actuation performances of PZT with AlN, one should increase of ~1 order of magnitude the piezoelectric film area or the driving voltage, resulting in high volume occupation (and die cost) or dedicated ASIC solution for high voltage driving which can be less efficient (increased area and power consumption).

One can argue that the power consumption of a PZT thin film is greater than AlN and AlScN due to higher relative permittivity and dielectric losses, but it is worth stressing that typical quasi-static PZT MEMS actuator have a capacitance in the range of 10-100nF, which translates in a power consumption well below 10mW (assuming 40V of driving voltage and up to 120Hz actuation frequency), almost negligible compared with the power consumption of other components of a projection system (driving electronics, lasers, …). In addition, the lower operating voltage (typical <50V) of PZT-based actuators requires less power-hungry electronics, resulting in an overall lower power consumption of the system.

AlN and AlScN can be more efficient in other kind of applications, such sensors, where its properties of higher linearity, stability and the lower permittivity can provide a high, linear and stable over time output voltage. The nonlinearity and variability over time (if not poled) of PZT thin films actuation require to monitor the device behavior during the lifetime. For the device presented in this work, a standard piezoresistive (PZR) sensor in Whetstone bridge configuration [17] has been used to sense the stress on the torsional springs, enabling the possibility to know the mirror position and to perform a closed loop control with the dedicated electronics. Finally, an additional characteristic has to be taken into account for the PZT case, that is its displacement response upon polarization: PZT is characterized by a typical butterfly-shaped electric field-to-displacement curve, which means that the imposed displacement has the same direction upon reversal of the electric field and consequent switch of the piezoelectric domains. Typical displacement curves for unipolar and bipolar polarization are reported in Figure 2 and a comprehensive treatment of PZT nonlinearities can be found in [11]. This could appear as an additional limitation of PZT with respect to the linear response of AlN, but it can be easily and effectively overcome by the mechanical design, as it will be shown in the following, by adopting actuators at opposite sides of the mirror rotation axis to generate opposite mirror tilt directions.

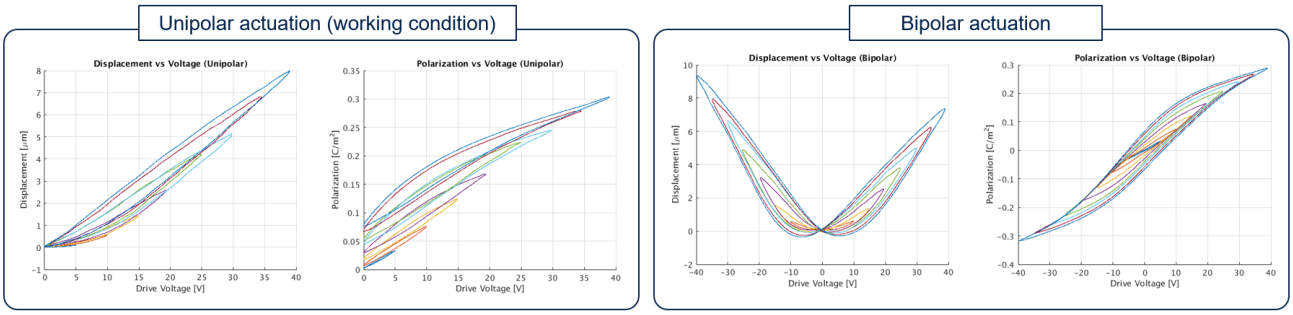

Figure 2 Unipolar (left) and bipolar (right) plots of displacement and polarization versus voltage, for different values of maximum voltage, collected on a cantilever structure. The plots highlight the nonlinear and hysteretic behavior of the PZT material, which is monitored using a PZR sensor. The bipolar plots show how the displacement is positive direction regardless the sign of the applied voltage, requiring PZT actuators on both sides of the MEMS mirror to obtain positive and negative rotation around the rotational axis.

Following these considerations, PZT has been selected as the material of choice for piezoelectric actuators in STMicroelectronics' proprietary PεTRA process platform [12]. In Figure 3 is reported the schematic process flow description with the main fabrication steps: the starting wafer is an SOI, where diffused piezoresistors are defined. The PZT stack, comprehensive of passivation, electrodes and routing metals is then realized, using the sol-gel process to deposit the PZT thin-film. The movable masses are patterned by means of a silicon DRIE process on the thinner top silicon layer and on the thicker backside silicon layer, used to define the external frame and the backside reinforcement under the mirror, to guarantee the mirror flatness. Lastly, the wafer is bonded with a second wafer (cap), pre-patterned with a cavity. The last step is not mandatory for the mirror functioning but makes the MEMS device robust during handling and simplify the assembly, since the cavity that enables the mirror movement is already defined during the wafer fabrication.

In the MEMS mirror described in this work aluminum material is used as reflective layer, thus optimized for visible projection (AR/MR, picoprojectors, …), but alternative reflecting metals could also be used in the same process platform for other applications, for example gold for 3D sensing or LiDAR systems.

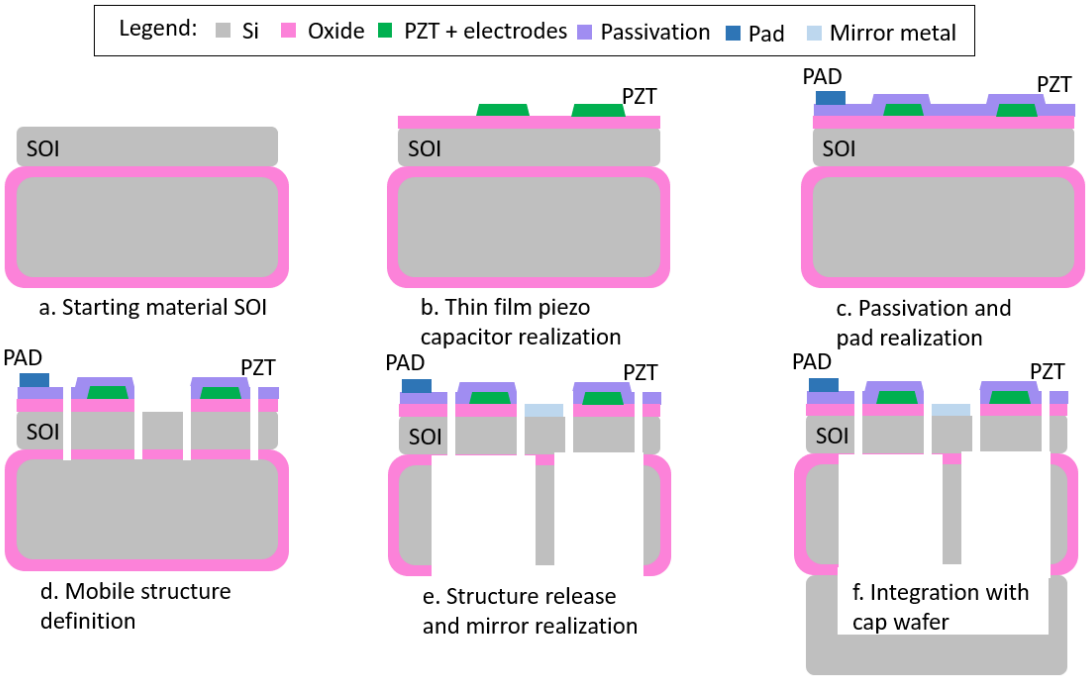

Figure 3 Schematic process flow description

The reflective area of the MEMS mirror is 4x3mm^2, significantly bigger than the solutions that can be found in literature (usually up to 2mm diameter [7]-[10][15][16]) and the overall die size is 11x5mm^2 with a remarkable 20% fill ratio of the mirror area. This solution offers great performances and small volume occupation for multiple applications: the big mirror area, coupled with a fast scanner, can be used to create high resolution images (>1080/1440p) for AR/VR or to increase the range of LiDAR systems beyond 200m.

The MEMS mirror layout is reported in Figure 4: in light blue are reported the reflective area (rotating around the x-axis) and the routing metals, in grey are represented the silicon structures, in yellow the PZR sensor and in green the PZT actuators. As per what described before, two piezoelectric actuators are required to generate the full mechanical scan angle: the two actuators are connected at opposite sides of the mirror rotation axis to generate opposite direction rotations even if PZT can support a displacement only along one direction, for this reason the actuators (which are exactly the same) are reported using different green scales. The two actuators are forced alternatively with fully-positive signals (e.g. sawtooth, triangular, sinusoidal…) in order to stay in the region where the voltage-to-displacement is most linear and to prevent the domain switching in the PZT material (as described in Figure 2) which in addition may affect the reliability of the actuators. As an example, in Figure 5 are reported the sawtooth driving waveforms on the two PZT actuator, with the resulting mirror motion and PZR sensor output.

The reflective area is connected to the anchor points using torsional springs, which allow the mirror rotation while reducing the vertical motion of the mirror. In addition, having the mirror connected directly to the anchor points by using these torsional springs is very important to increase the robustness against shock of the device, a key feature for consumer and automotive applications. At the anchor point of one torsional spring is placed the PZR sensor which, as reported in Figure 5, allows to have a correlation between the mirror torsional movement and the sensing voltage. The reflective area is then connected to the actuators by means of folded springs, which uncouple the mirror rotation with the actuator curvature, another key feature of this design concept since it allows to use the high out-of-plane force of the PZT actuators without being affected by its deformed shape.

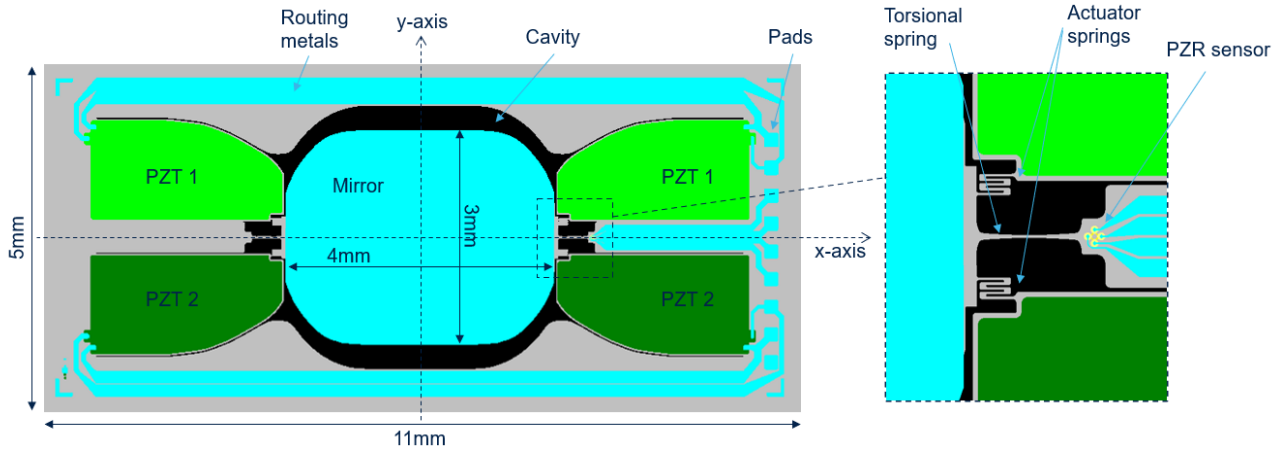

Figure 4 MEMS mirror design description

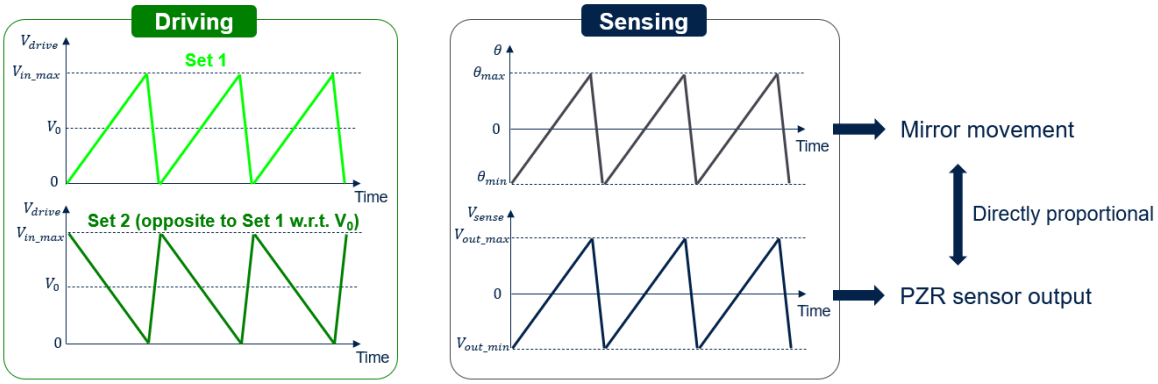

Figure 5 Input driving voltage on the two actuator sets (left) with the resulting mirror movement and PZR sensor output (right)

In Figure 6 is reported a comparison between the novel design concept used in this work and one of the standard approaches that can be found in literature [16]: it can be noted how in this design the connection point between the actuators and the mirror is placed near the rotational axis, reducing the out-of-plane movement required by the PZT actuators and exploiting a lever mechanism that enable large rotations of the mirror with relatively short PZT actuators. On the contrary, in the standard design concept, the required out-of-plane movement of the actuator is equal to the movement of the mirror tip, which affect the device efficiency thus requiring several folded actuators in series to reach the desired opening angle (from 5deg up to 15deg half mechanical scan angle are usually required). In addition, as reported above, the adopted solution uses two torsional springs that directly connect the reflective area with the anchor point, which increase the robustness and the resonant frequencies of the unwanted spurious modes (e.g. out-of-plane pumping mode, in-plans translational modes).

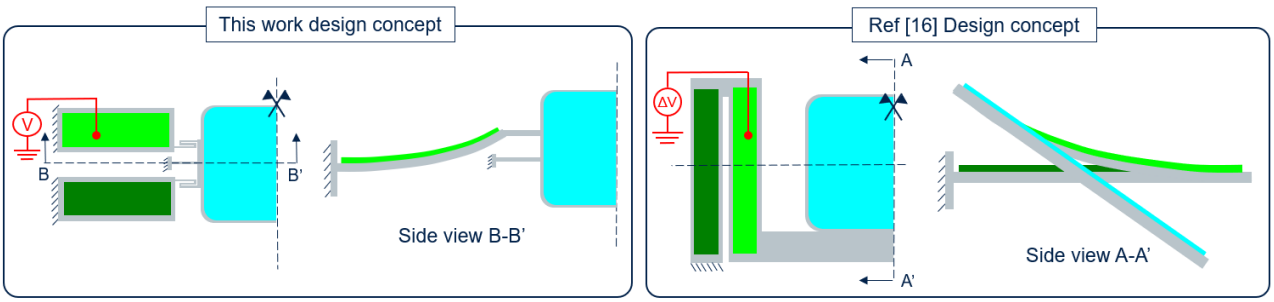

Figure 6 Patented design (left) and state-of-the art (right) design concepts working principle

3. SIMULATION AND EXPERIMENTAL RESULTS

Finite element (FEM) simulations have been performed in the design phase to predict the main functioning parameters (opening angle, modal behavior, PZR sensor sensitivity, shock robustness …) of the device. The target half mechanical opening angle was of 8deg, considering an operative maximum peak voltage of 40V. In Figure 7 are reported the simulated displacements and the stresses, considering a 40V voltage applied on PZT actuator 1 (as reported in Figure 4) and 0V voltage applied on PZT actuator 2. The simulated half mechanical opening angle (~9deg) is slightly higher with respect to the target value of 8deg, which guarantees a minimum opening angle of 8deg considering possible process spreads. The maximum of the first principal stress component is ~0.9GPa, located in the springs that connect the reflective area to the actuators, this value is well below the Si limit of about 3GPa [18][19].

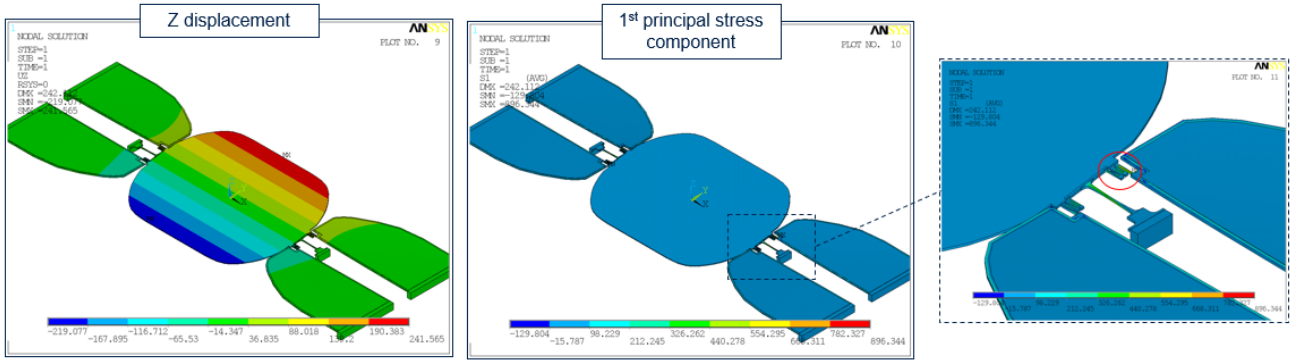

Figure 7 FEM simulation results: displacements (left) and stresses (right) with 40V actuation voltage and ~9deg half mechanical angle. Maximum stress (~0.9GPa) location highlighted in the red circle.

The results of the modal analysis are reported in Figure 8: the first (torsional) mode is located at 565Hz and its deformation is aligned with the quasi-static deformation in working conditions. The goal was to have the 1st mode frequency higher than 500Hz, to successfully drive the mirror in closed loop and limiting the unwanted excitation arising from nonlinearities and sharp points of sawtooth and triangular driving waveforms. Other important parameters are the frequencies of the spurious modes, which are directly related to the stiffness and thus to robustness of the device for Y and Z translations. With this design the 1st spurious mode (Z-translation) has a resonant frequency >3kHz, which highlight the high robustness of the device against external excitation, as will be shown below with shock simulations and tests.

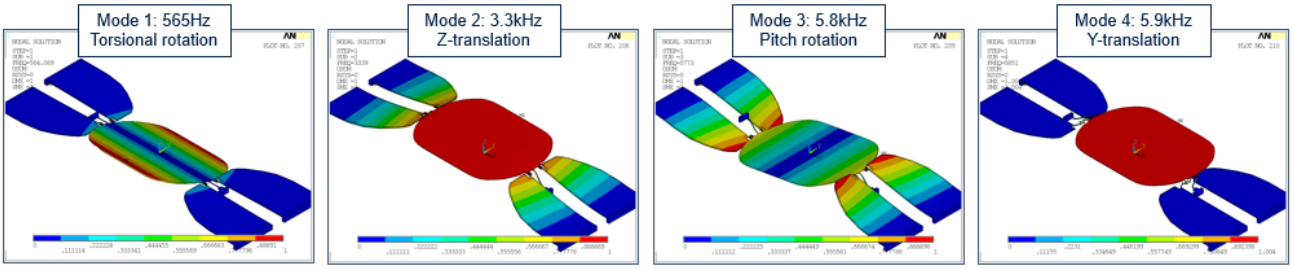

Figure 8 Modal analysis up to 6kHz

To perform experimental tests the MEMS mirror a dedicated PCB has been developed to simplify the handling and reducing the testing time. In Figure 9 are reported some images of the package used and the description of the test setup: the PCB is placed in a board using the card-edge connector, perpendicular to a laser source which is deflected by the MEMS reflective area on a perforated sheet. A camera collects the length of projection and by knowing the distance between the MEMS and the sheet is possible to obtain the opening angle of the mirror. In addition, the output voltage from the PZR sensor is collected by an oscilloscope to check the PZR sensor sensitivity. All the measurements are performed automatically, using a PC with a dedicated software.

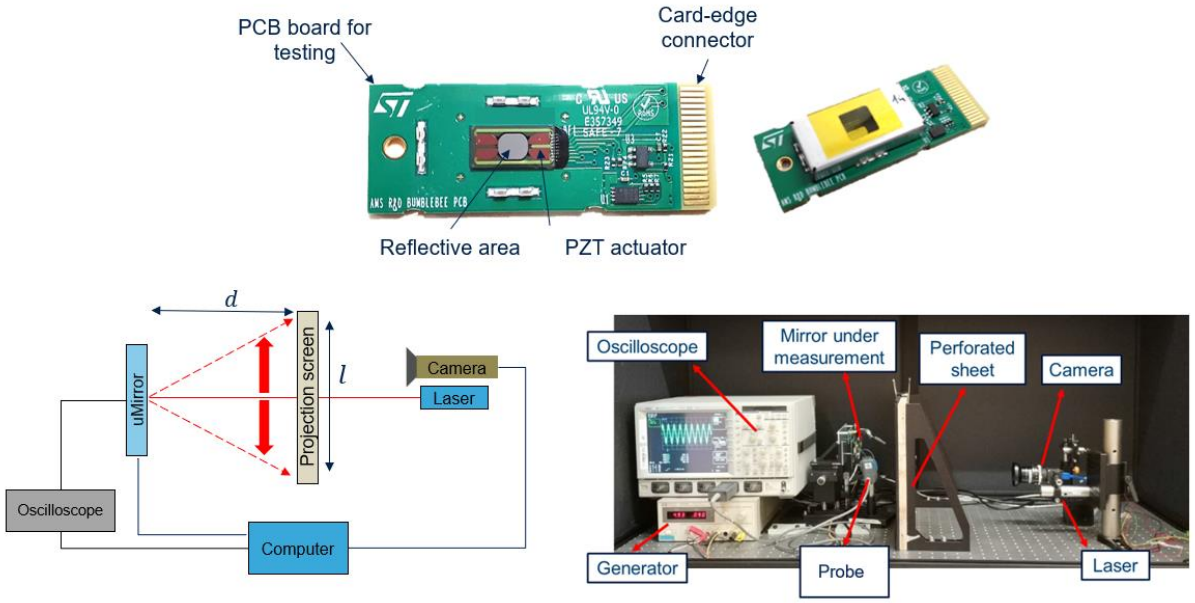

Figure 9 Details of the PCB and experimental setup used to test the MEMS mirror

The results of FEM nonlinear static simulations are compared with the experimental results obtained on 3 samples in Figure 10, for different values of peak driving voltage. The half mechanical opening angle θ is reported in the plot and it is useful to underline that the resultant field of view (FOV) is 4xθ, 36deg considering an 9deg half mechanical opening angle at 40V. The correlation between experimental and simulated results is remarkable across the entire voltage range. As highlighted previously, the maximum voltage in operating conditions is 40V, but in the characterization phase the samples have been stressed up to 80V (deformed configuration shown in Figure 11) to check the margin with respect possible silicon breakages. An excellent result has been obtained since no breakages have been found up to almost double stress with respect to the target angle. The source of the nonlinearity that become significant over 10deg is mainly mechanical, related to the deformation of the springs that connects the reflective area to the actuators. In the same measurements also the PZR sensor sensitivity is measured, showing a good agreement between experimental (average value of 1.3mV/V/deg) and simulated data (1.4mV/V/deg, where mV is the output of the sensor for each V of bias voltage given to the Wheatstone bridge for each degree of rotation of the mirror).

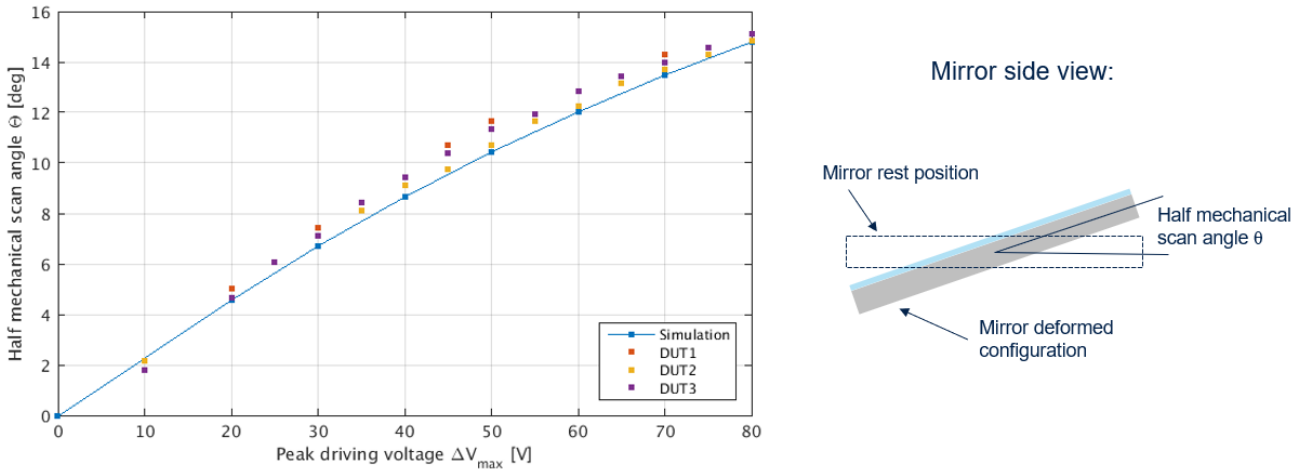

Figure 10 Opening angle vs peak driving voltage: simulation vs experimental results. On the right is reported the definition of half mechanical scan angle θ, the mechanical opening angle is then 2xθ and the resultant field of view (FOV) of the projection is 4xθ

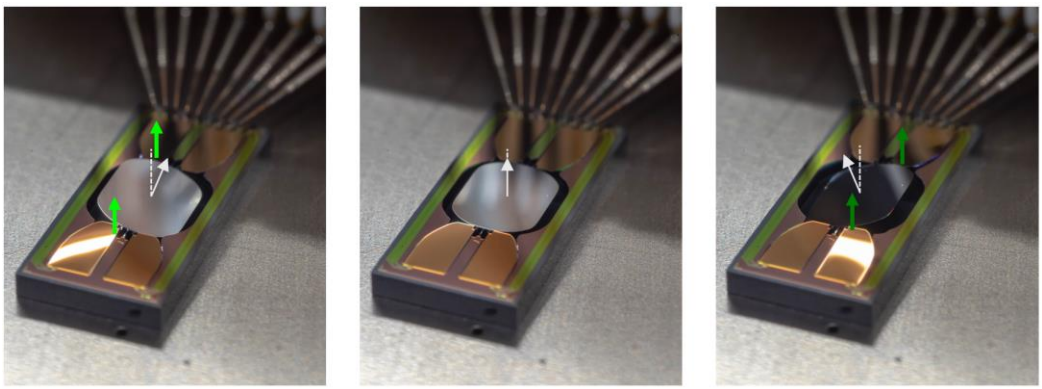

Figure 11 Image of the MEMS scanner with 80V applied on PZT actuators 1 and 0V applied on PZT actuators 2 (left), in rest condition (center) and with 80V applied on PZT actuators 2 and 0V applied on PZT actuators 1 (right).

The modal behavior is then studied experimentally using a Polytec MSA-500 vibrometer analyzer [20], the results are shown in Figure 12. The first torsional mode is found at 570Hz, in excellent agreement with the simulated value of 565Hz, while the Z-translation mode is found at 3.2kHz, aligned with the simulated value of 3.3kHz. Due to the metal routing configuration it is not possible to see the third mode of Figure 8, since PZT actuators belonging to the same set cannot be actuated in opposite phase, as the mode would require, since they are connected by metal routings. The last mode below 6kHz found in the simulations is the Y-translation mode, which is not present in graph because it is an in-plane mode and it cannot be measured by using a vibrometer.

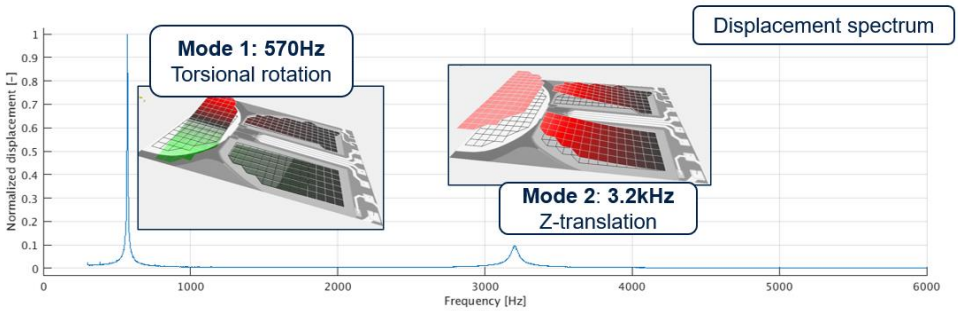

Figure 12 Experimental modal analysis, obtained using a vibrometer

After the design validation tests shown above, the devices have been tested with operative conditions of cyclic 0-40V driving voltage in open loop for 168 hours, collecting the PZR sensor signal as shown in Figure 13 for a couple of samples. The aim of this test is to check the MEMS reliability and identify possible failure mechanisms and design weaknesses: the opening angle appears stable even in open loop driving conditions and no mechanical or electrical failures are observed, confirming the robustness of this design solution.

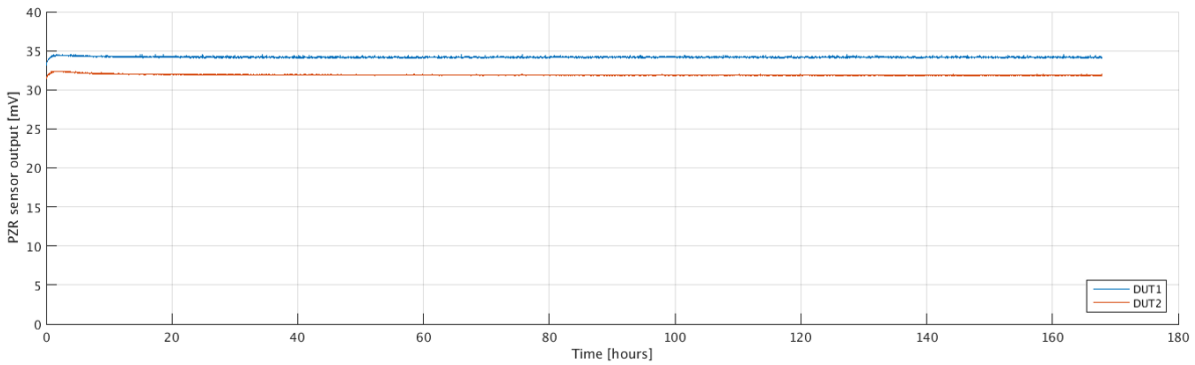

Figure 13 Opening angle stability over time at constant driving voltage (open-loop actuation)

Another important design parameter for such big MEMS components is related to the shock robustness of the device, which may become the most critical design parameter for consumer and automotive applications. Before the device manufacturing, FEM shock simulations have been performed, considering the test conditions reported in MIL-STD-883E [21] shown in Table 2.

Table 2 Shock conditions reported in MIL-STD-883E

Acceleration peak [g]	Pulse width [ms]
500	1
1500	0.5
3000	0.3

The minimum shock robustness usually required for MEMS mirror components is 500g, while for some applications it is required a shock robustness of 1000 or 1500g. During the design phase of the device presented in this work, the goal was to achieve a shock robustness of 1500g: Figure 14 shows the simulation results of a shock in Z direction (the most critical, perpendicular to the mirror plane) with 1500g peak acceleration and 0.5ms pulse width. The maximum out of plane displacement of the mirror is limited to about 50µm and the maximum principal stress is of about 1.3GPa, well below the already mentioned silicon limit which is ~3GPa.

These results are confirmed by the experimental activity: 10 samples have been tested with cumulated shock conditions at increasing shock amplitude of 500g, 1500g and 3000g (10 shock repeated in X, 10 in Y and 10 in Z direction for each shock amplitude). No breakage is found for input accelerations of 500g and 1500g, while some broken samples are found after 3000g, where the expected stress on the silicon spring is near the material limit.

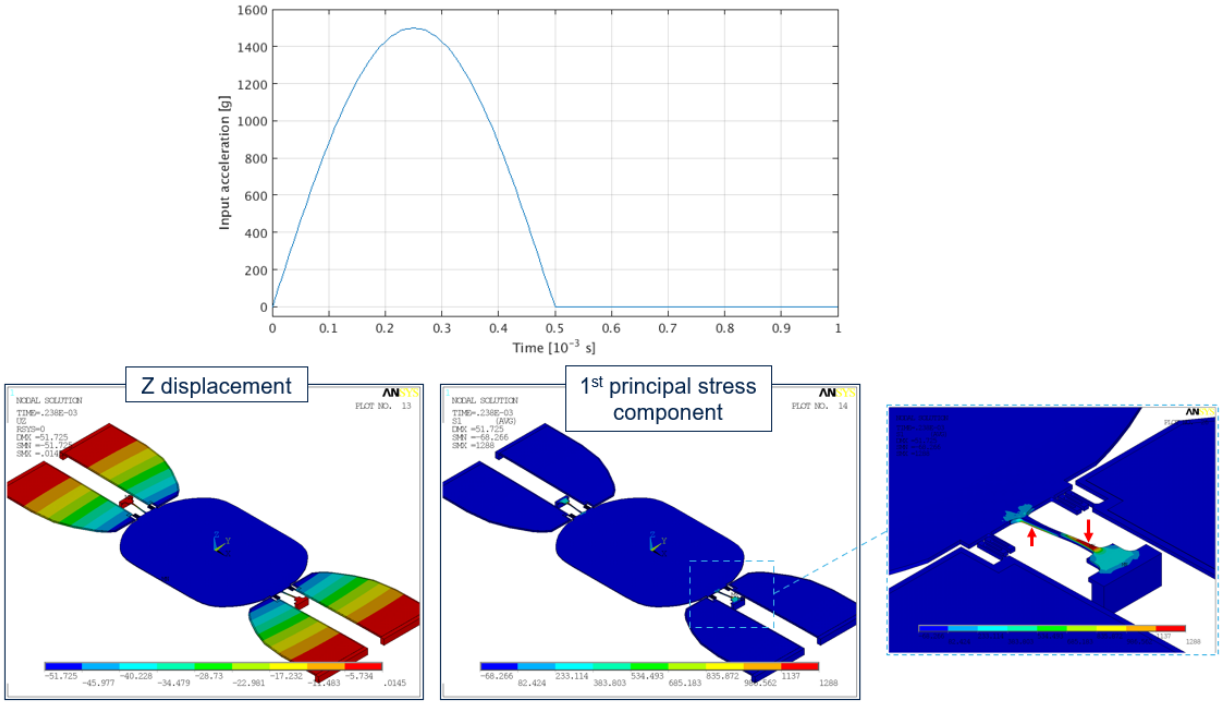

Figure 14 Shock simulation results: half sine input acceleration of 1500g with 0.5ms pulse width (top) as per MIL-STD-883E, out of plane resultant displacement (left) and first principal stress component (right). Maximum stress locations highlighted by red arrows (top and bottom faces of central torsional springs).

In Figure 15 is shown a sample before and after the 3000g test: it can be noted that the crack on the silicon spring is located in the same position of the maximum stress (red arrow) in the simulation results of Figure 14. One can also note that after the spring crack, the successive shocks lead to a catastrophic failure of the device, with the breakage of the springs that

connect the reflective area to the actuators and the consequent removal of the mirror (white area in the left image, absent in the right image).

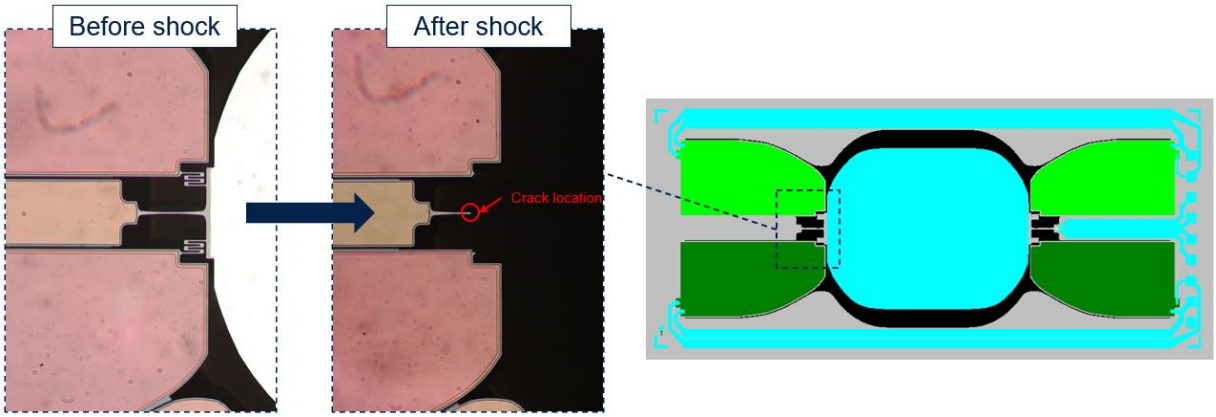

Figure 15 Image of torsional spring location before and after a shock test of 3000g, 0.3ms pulse width (left) and layout reference (right). Crack location aligned with the maximum stress location obtained in simulations, shown in Figure 14.

4. CONCLUSIONS

In this work, a quasi-static MEMS mirror with PZT actuation has been thoroughly analyzed: from the reasons behind the piezoelectric material selection, going through the simulations and design validation data and finally presenting the main reliability tests results. The device shows remarkable results in terms of performance, providing a big reflective area of 4x3mm^2 with an opening angle up to 15deg (~9deg considering the target driving voltage of 40V) in a compact die size while fulfilling the robustness requirements for consumer and automotive applications. Starting from this design concept and process platform it is possible to build similar MEMS mirrors optimized for specific use cases: by reducing the reflective area (which may be overdesigned for most applications), it is possible to increase the opening angle or reduce the overall MEMS footprint. In addition, improvements of the PZT process platform adopted in this work are under development and may provide up to a 2 times more efficient material in terms of torque, which will further increase the reachable opening angles and reflective area while reducing the volume occupation of the device.

Acknowledgements

The authors wish to thank Stefano Losa (STMicroelectronics MEMS Q&R) for the support in the MEMS reliability testing, Sonia Costantini (STMicroelectronics MEMS R&D) for the support in the description of the technology manufacturing process and all the MEMS technology R&D team working at STMicroelectronics in Agrate (Italy) for providing the microfabrication of the device.

REFERENCES

[1] North: https://www.bynorth.com/
[2] Microsoft Hololens 2: https://www.microsoft.com/en-us/hololens
[3] Bosch Smartglasses Light Drive module: https://www.bosch-sensortec.com/news/smartglasses.html
[4] Intel RealSense L515: https://www.intelrealsense.com/lidar-camera-l515/
[5] Innoviz One: https://innoviz.tech/innovizone
[6] Bernard Kress, "Optical Architectures for Augmented-, Virtual-, and Mixed-Reality Headsets", SPIE (2020) https://doi.org/10.1117/3.2559304
[7] Ulrich Hofmann, Sascha Muehlmann, Martin Witt, Klaus Doerschel, Rijk Schuetz, and Bernd Wagner "Electrostatically driven micromirrors for a miniaturized confocal laser scanning microscope", Proc. SPIE 3878, Miniaturized Systems with Micro-Optics and MEMS, (2 September 1999); https://doi.org/10.1117/12.361269

[8] J Jin-Woo Cho, Yong-Hwa Park, Young-Chul Ko, Byeung-Leul Lee, Seok-Jin Kang, Seok-Whan Chung, Won-kyoung Choi, Yong-Chul Cho, Seok-Mo Chang, Jin-Ho Lee, and John Sunu "Electrostatic 1D microscanner with vertical combs for HD resolution display", Proc. SPIE 6466, MOEMS and Miniaturized Systems VI, 64660B (22 January 2007); https://doi.org/10.1117/12.702163
[9] Yunfei Ma, Wyatt O. Davis, Matt Ellis, and Dean Brown "Nonlinear mathematical model for a biaxial MOEMS scanning mirror", Proc. SPIE 7594, MOEMS and Miniaturized Systems IX, 75940B (16 February 2010); https://doi.org/10.1117/12.843084
[10] Chang-Hyeon Ji, Moongoo Choi, Sang-Cheon Kim, Ki-Chang Song, Jong-Uk Bu; Hyo-Jin Nam "Electromagnetic Two-Dimensional Scanner Using Radial Magnetic Field", Journal of Microelectromechanical Systems, Vol.16, No.4, August 2007; https://doi.org/10.1109/JMEMS.2007.892897
[11] Attilio Frangi, Andrea Opreni, Nicolò Boni, Patrick Fedeli, Roberto Carminati, Massimiliano Merli, Gianluca Mendicino "Nonlinear Response of PZT-Actuated Resonant Micromirrors," in Journal of Microelectromechanical Systems, Vol. 29, No. 6, pp. 1421-1430, Dec. 2020, https://doi.org/10.1109/JMEMS.2020.3022557
[12] STMicroelectronics PεTRA technology platform: https://investors.st.com/news-releases/news-release-details/stmicroelectronics-and-usound-deliver-first-advanced-mems
[13] Polight: https://www.polight.com/home/default.aspx
[14] USound: https://www.usound.com/
[15] S. Gu-Stoppel, T. Lisec, M. Claus, N. Funck, S. Fichtner, S. Schröder, B. Wagner, and F. Lofink "A triple-wafer-bonded AlScN driven quasi-static MEMS mirror with high linearity and large tilt angles", Proc. SPIE 11293, MOEMS and Miniaturized Systems XIX, 1129304 (28 February 2020); https://doi.org/10.1117/12.2542800
[16] Tomotaka Asari, Takaaki Koyama, Masanao Tani, Hiroshi Toshiyoshi "A Bi-Axial Piezoelectric MEMS Scanning Mirror for Automobile Lighting System", 2019 International Conference on Optical MEMS and Nanophotonics (OMN); https://doi.org/10.1109/OMN.2019.8925159
[17] Enri Duqi, Lorenzo Baldo, Mikel Azpeitia Urquia, Giorgio Allegato "A Piezoresistive Mems Barometer with Thermomecanical Stress Rejection", 2019 20th International Conference on Solid-State Sensors, Actuators and Microsystems & Eurosensors XXXIII (TRANSDUCERS & EUROSENSORS XXXIII); https://doi.org/10.1109/TRANSDUCERS.2019.8808357
[18] E.K. Baumert, P.-O. Theillet, O.N. Pierron, "Investigation of the low-cycle fatigue mechanism for micron-scale monocrystalline silicon films", Acta Materialia, Vol. 58, No. 8, pp. 2854-2863, 2010; https://doi.org/10.1016/j.actamat.2010.01.011
[19] Alexander Wolter, Harald Schenk, Hilmar Korth, and Hubert Lakner "Torsional stress, fatigue and fracture strength in silicon hinges of a micro scanning mirror", Proc. SPIE 5343, Reliability, Testing, and Characterization of MEMS/MOEMS III, (23 December 2003); https://doi.org/10.1117/12.524872
[20] Polytec MSA-500: https://www.polytec.com/fileadmin/d/Vibrometrie/OM_BR_MSA-500_E_42121.pdf
[21] MIL-STD-883, [TEST METHOD STANDARD MICROCIRCUITS], US Department of Defense (1996)